Behavioral/Systems/Cognitive

Mobilization of Calcium from Intracellular Stores Facilitates Somatodendritic Dopamine Release

Jyoti C. Patel,[1] Paul Witkovsky,[2] Marat V. Avshalumov,[1] and Margaret E. Rice[1,3]

Departments of [1]Neurosurgery, [2]Ophthalmology, and [3]Physiology and Neuroscience, New York University School of Medicine, New York, New York 10016

Somatodendritic dopamine (DA) release in the substantia nigra pars compacta (SNc) shows a limited dependence on extracellular calcium concentration ($[Ca^{2+}]_o$), suggesting the involvement of intracellular Ca^{2+} stores. Here, using immunocytochemistry we demonstrate the presence of the sarcoplasmic/endoplasmic reticulum Ca^{2+}-ATPase 2 (SERCA2) that sequesters cytosolic Ca^{2+} into the endoplasmic reticulum (ER), as well as inositol 1,4,5-triphosphate receptors (IP_3Rs) and ryanodine receptors (RyRs) in DAergic neurons. Notably, RyRs were clustered at the plasma membrane, poised for activation by Ca^{2+} entry. Using fast-scan cyclic voltammetry to monitor evoked extracellular DA concentration ($[DA]_o$) in midbrain slices, we found that SERCA inhibition by cyclopiazonic acid (CPA) decreased evoked $[DA]_o$ in the SNc, indicating a functional role for ER Ca^{2+} stores in somatodendritic DA release. Implicating IP_3R-dependent stores, an IP_3R antagonist, 2-APB, also decreased evoked $[DA]_o$. Moreover, DHPG, an agonist of group I metabotropic glutamate receptors (mGluR1s, which couple to IP_3 production), increased somatodendritic DA release, whereas CPCCOEt, an mGluR1 antagonist, suppressed it. Release suppression by mGluR1 blockade was prevented by 2-APB or CPA, indicating facilitation of DA release by endogenous glutamate acting via mGluR1s and IP_3R-gated Ca^{2+} stores. Similarly, activation of RyRs by caffeine increased $[Ca^{2+}]_i$ and elevated evoked $[DA]_o$. The increase in DA release was prevented by a RyR blocker, dantrolene, and by CPA. Importantly, the efficacy of dantrolene was enhanced in low $[Ca^{2+}]_o$, suggesting a mechanism for maintenance of somatodendritic DA release with limited Ca^{2+} entry. Thus, both mGluR1-linked IP_3R- and RyR-dependent ER Ca^{2+} stores facilitate somatodendritic DA release in the SNc.

Introduction

Nigrostriatal neurons release dopamine (DA) from their somata and dendrites in the substantia nigra (SN) pars compacta (SNc) and pars reticulata (SNr) (Björklund and Lindvall, 1975; Geffen et al., 1976; Nieoullon et al., 1977; Cheramy et al., 1981; Robertson et al., 1991; Rice et al., 1994; Jaffe et al., 1998), as well as from their axons in striatum. The understanding of somatodendritic release is incomplete at present. Release of nigral DA is sensitive to tetrodotoxin (TTX) (Santiago et al., 1992; Chen and Rice, 2001), VMAT2 inhibitors (Rice et al., 1994; Heeringa and Abercrombie, 1995; Beckstead et al., 2004), botulinum toxins (Bergquist et al., 2002; Fortin et al., 2006), and exhibits a limited dependence on extracellular calcium concentration ($[Ca^{2+}]_o$) (Chen and Rice, 2001). These observations are consistent with Ca^{2+}-dependent exocytosis. However, the source(s) of Ca^{2+} underlying somatodendritic DA release remains undefined.

Neurotransmitter release typically is triggered by a rise in intracellular Ca^{2+} concentration ($[Ca^{2+}]_i$), primarily from Ca^{2+} influx through voltage-gated Ca^{2+} channels (VGCCs). However, unlike axonal DA release, somatodendritic DA release in SNc persists in submillimolar $[Ca^{2+}]_o$ (Hoffman and Gerhardt, 1999; Chen and Rice, 2001; Fortin et al., 2006) and is resistant to the effects of VGCC blockers at concentrations sufficient to abolish striatal release (Elverfors et al., 1997; Chen et al., 2006). These data imply that somatodendritic DA release requires minimal Ca^{2+} entry and suggest the involvement of intracellular Ca^{2+} stores.

Increasing evidence implicates Ca^{2+} release from endoplasmic reticulum (ER) stores in transmitter release (Krizaj et al., 1999; Emptage et al., 2001; Bardo et al., 2002; Simkus and Stricker, 2002; Galante and Marty, 2003), including dendritic secretion of oxytocin and vasopressin from hypothalamic neurons (Ludwig et al., 2002; Bergquist and Ludwig, 2008) and somatic release of serotonin from Retzius cells (Trueta et al., 2004). These Ca^{2+} stores are maintained by the sarcoplasmic/endoplasmic reticulum Ca^{2+}-ATPase (SERCA), which sequesters cytosolic Ca^{2+} into the ER (Pozzan et al., 1994; Verkhratsky, 2005). Release of Ca^{2+} from ER stores occurs via two Ca^{2+} release channels: inositol 1,4,5-triphosphate receptors (IP_3Rs), which are activated by metabotropic receptor-dependent IP_3 production (Foskett et al., 2007), and ryanodine receptors (RyRs), which are activated by Ca^{2+} in a process of Ca^{2+}-induced Ca^{2+} release (CICR), as well as by a change in membrane voltage (Verkhratsky and Shmigol, 1996; Fill and Copello, 2002).

In SNc DAergic neurons, Ca^{2+} release from IP_3R-gated stores after transient activation of group I metabotropic glutamate receptors (mGluR1s) or from RyR-gated stores regulates cell excitability (Fiorillo and Williams, 1998; Tsuneki et al., 2000;

Received Jan. 12, 2009; revised March 17, 2009; accepted March 27, 2009.

This work was supported by National Institutes of Health–National Institute of Neurological Disorders and Stroke Grant NS-36362 (M.E.R.), the Attilio and Olympia Ricciardi Research Fund (M.E.R.), and the Richard H. Chartrand Foundation (P.W.).

Correspondence should be addressed to Dr. Margaret E. Rice, Department of Physiology and Neuroscience, New York University School of Medicine, 550 First Avenue, New York, NY 10016. E-mail: margaret.rice@nyu.edu.

M. V. Avshalumov's present address: Department of Neurosurgery, Mount Sinai Medical Center, New York, NY 10029.

DOI:10.1523/JNEUROSCI.0181-09.2009

 0270-6474/09/296568-12$15.00/0

Table 1. Primary antibodies

Antibody	Source	Catalog no.	Species	Dilution (fold)
$Ca_v1.3$	Sigma	C1728	Rabbit	500
Calbindin	Sigma	C-8666	Mouse	1000
IP_3R	Millipore Bioscience Research Reagents	MAB3078	Mouse	1000–2000
mGluR1α	Millipore Bioscience Research Reagents	AB1551	Rabbit	200–500
RyR	Affinity BioReagents	MA3-925	Mouse	500
SERCA2	Affinity BioReagents	MA3-910	Mouse	1500–2000
TH	Millipore Bioscience Research Reagents	MAB318	Mouse	500
TH	Millipore Bioscience Research Reagents	AB152	Rabbit	800

Morikawa et al., 2003). The role that ER Ca^{2+} stores play in somatodendritic DA release in SNc, however, is unknown. Using immunocytochemistry with confocal microscopy, we identified proteins that regulate ER Ca^{2+} stores, including SERCA, IP_3Rs, RyRs, and mGluR1s, in DAergic somata and dendrites in the SN. We then used fast-scan cyclic voltammetry in midbrain slices to assess the functional roles of these proteins in somatodendritic DA release in SNc. These studies reveal that Ca^{2+} release from IP_3R- and RyR-gated ER stores facilitates somatodendritic DA release.

Materials and Methods

Animals. All animal handling procedures were in accordance with National Institutes of Health guidelines and were approved by the New York University School of Medicine Animal Care and Use Committee. Young adult guinea pigs (male, Hartley, 150–250 g) were obtained from Charles River Laboratories) and were deeply anesthetized with an intraperitoneal injection of sodium pentobarbital (50 mg/kg). Guinea pigs were chosen as the experimental animal for these studies because voltammetric measurements detect a pure DA release response in guinea-pig SNc (Rice et al., 1994, 1997; Cragg et al., 1997a,b), whereas DA release in the SNc of rats and mice is masked by concurrently released serotonin (Rice et al., 1994; Iravani and Kruk, 1997; Cragg et al., 1997b; John et al., 2006). Similarly, all voltammetric studies were done in SNc, rather than SNr, as serotoninergic input to the distal dendrites of nigral DAergic neurons precludes voltammetric monitoring of pure DA release in the SNr (Rice et al., 1994; Cragg et al., 1997b).

Preparation of fixed, frozen midbrain sections. Anesthetized guinea pigs were perfused transcardially with PBS (9.0 g/L NaCl in 10 mM phosphate buffer, pH 7.3) followed by freshly prepared paraformaldehyde (4%) in PBS. The brain was then removed and immersed in this fixative for 1 h. A coronal block of midbrain was dissected free and washed in PBS for 30 min, then placed for 16–24 h in 30% sucrose in PBS for cryoprotection. Coronal sections (20 μm) through the anterior midbrain were cut on a Reichert-Jung Cryocut 1800 cryostat (Belair Instrument Company), mounted on slides, dried for 1 h at 37°C, then stored at −20°C until use. Patterns of immunolabeling for some intracellular proteins in DAergic neurons were compared with those in cerebellar Purkinje cells. For these studies, cerebellar sections (20 μm) were prepared in the same manner as midbrain sections. Purkinje cells were identified by their characteristic shape and their immunoreactivity to anti-calbindin D28 (not illustrated).

Immunocytochemistry. Slides were washed 3 times for 7 min each (3 × 7 min) in PBS and 30 min in blocking solution [10 ml of PBS, containing 0.1 g of bovine serum albumin, 30 μl of Triton X-100 and 100 μl of 10% (w/v) Na-azide], then incubated in a mixture of primary antibodies for 16–20 h at room temperature. After a further 3 × 7 min wash in PBS, sections were exposed to secondary antibodies Alexa 488 (Invitrogen) and Cy3 (Jackson Immunoresearch) for 2 h. After a final 3 × 7 min wash in PBS, sections were coverslipped in VectaShield (Vector Labs). No immunostaining was observed when the primary antibodies were omitted.

Fluorescent images were obtained with a Nikon PM 800 confocal microscope equipped with a digital camera controlled by the Spot software program (Diagnostic Instruments). Digital images were acquired separately from each laser channel, then recombined. Digital files were processed with deconvolution software (AutoQuant Imaging). Adobe Photoshop 7.0 was used to further process digital images. Any adjustments to brightness and contrast were made uniformly to all parts of the image.

Antibodies and their specificity. A list of the primary antibodies used, their sources and effective dilutions is provided in Table 1. Polyclonal anti-$Ca_v1.3$ was raised in rabbit against a synthetic peptide of amino acids 859–875 of the α unit of rat $Ca_v1.3$ (Swiss-Prot, accession number P27732). In immunoblots of rat brain, this antibody recognizes the α subunit of $Ca_v1.3$ (Hell et al., 1993). Mouse monoclonal anti-calbindin was made against purified 28 kDa calbindin-D purified from chicken gut and stains the ^{45}Ca binding spot of calbindin-D in an immunoblot (manufacturer's specifications). Immunoreactivity is lost in a calbindin knock-out mouse, confirming specificity (Kriegsfeld et al., 2008). Mouse monoclonal anti-IP_3R was raised against a synthetic polypeptide KDSTEYTGPESYV coupled through a terminal cysteine to keyhole limpet hemocyanin (KLH). In immunoblots, this antibody recognized IP_3Rs purified from rat brain (Bourguignon et al., 1993). Rabbit anti-mGluR1α was raised against the carboxy terminal peptide (PNVTYASVILRDYKQSSSTL) of rat mGluR1α conjugated to KLH with glutaraldehyde. This antibody recognizes a single band of 140 kDa in retina, corresponding to the M_r of mGluR1α (Koulen et al., 1997). Immunoreactivity was blocked by preadsorption of the antibody with its antigenic peptide. Mouse monoclonal anti-RyR was raised against partially purified chicken pectoral muscle RyR and recognizes all three isoforms of RyR in mouse tissue (manufacturer's specifications). In immunoblots of rat skeletal muscle extracts this antibody detects a band corresponding to the RyR (Stutzmann et al., 2006). Mouse monoclonal anti-SERCA2 ATPase was raised against purified canine cardiac sarcoplasmic reticulum and recognizes both isoforms of SERCA2. This antibody immunostains a band at 110 kDa from canine skeletal muscle triads corresponding to the SERCA protein (manufacturer's specifications). Mouse monoclonal anti-tyrosine hydroxylase (TH) was raised against purified TH from PC12 cells and immunostains only catecholaminergic neurons in brain (Beltramino et al., 1996) and only DAergic neurons in rodent retina (Witkovsky et al., 2005). Rabbit polyclonal anti-TH was raised against denatured (by SDS) TH from rat pheochromocytoma; in immunoblots it recognizes purified TH and immunostains only DAergic neurons in rodent retina (Witkovsky et al., 2005).

Preparation of acute midbrain slices. Procedures for preparing midbrain slices for voltammetry or imaging were according to those described previously by Avshalumov et al. (2005). Anesthetized guinea pigs were perfused transcardially with ~30 ml of ice-cold modified artificial CSF (aCSF) containing (in mM): sucrose (225), KCl (2.5), $CaCl_2$ (0.5), $MgSO_2$ (7), $NaHCO_3$ (28), NaH_2PO_4 (1.25), glucose (7), ascorbate (1) and pyruvate (3), and saturated with 95% O_2/5% CO_2. After perfusion, animals were decapitated and the brain rapidly removed and immersed in ice-cold modified aCSF for 1–2 min. The midbrain was then blocked in a coronal plane, fixed to the stage of a vibratome (Ted Pella) and sliced. Slices of midbrain (350 μm thick) were held at room temperature for at least 1 h before experimentation in HEPES-buffered aCSF containing (in mM): NaCl (120), KCl (5), $NaHCO_3$ (20), HEPES acid (6.7), HEPES salt (3.3), $MgSO_2$ (2), glucose (10); $CaCl_2$ (2) and saturated with 95% O_2/5% CO_2.

Voltammetric DA recording. For recording, slices were transferred to a submersion chamber (Warner Instruments) maintained at 32°C and su-

perfused at 1.2 ml/min with bicarbonate-buffered aCSF containing (in mM): NaCl (124); KCl (3.7); $NaHCO_3$ (26); $MgSO_2$ (1.3); KH_2PO_4 (1.3); glucose (10); $CaCl_2$ (2.4, unless noted otherwise) and saturated with 95% O_2/5% CO_2. After an equilibration period of at least 30 min, fast-scan cyclic voltammetry with carbon fiber electrodes was used to monitor extracellular DA concentration ($[DA]_o$) evoked by local electrical stimulation in the SNc as described previously (Chen and Rice, 2001, 2002; Chen et al., 2006; Patel and Rice, 2006).

Carbon-fiber electrodes were manufactured according to methods modified from Millar and Pelling (2001). After pulling, the carbon fiber (7 μm diameter, grade 34–700, un-sized, Goodfellows) was cut to a length of 30–70 μm from the glass seal using a mounted scalpel blade. Electrical contact with the carbon fiber was made using Woods metal (Goodfellows). Fast-scan cyclic voltammetry measurements were made using a Millar voltammeter (available by special request to Dr. Julian Millar at St. Bartholomew's and the Royal London School of Medicine and Dentistry, University of London, UK). The scan range was −0.7 V to + 1.3 V (vs Ag/AgCl), scan rate was 800 V/s, and the sampling interval was 100 ms. Identification of released DA was based on voltammograms with single oxidation and reduction peak potentials that define the voltammetric signature of DA (Patel and Rice, 2006). Evoked $[DA]_o$ was quantified by postexperimental calibration of carbon-fiber electrodes with known concentrations of DA at 32°C in control and all drug containing media used for a given experiment.

Somatodendritic DA release was evoked using a bipolar platinum-wire stimulating electrode positioned on the surface of the slice parallel to the band of cell bodies and lateral dendrites in the SNc. Evoked release was monitored at a carbon-fiber microelectrode positioned between the poles of the stimulating electrode, as described previously (Rice et al., 1997; Chen et al., 2001). The stimulation paradigm was a train of 30 pulses (0.6–0.8 mA pulse amplitude, 0.1 ms pulse duration) delivered at 10 Hz. This protocol allows examination of the consequences of concurrently released glutamate (Chen and Rice, 2002) and was essential in the present studies for assessment of the role of endogenously released glutamate in mGluR1-dependent activation of IP_3R-mediated Ca^{2+} stores.

In SNc, maximal evoked $[DA]_o$ is seen with an initial pulse-train stimulus, with a progressive decrease in amplitude with repetition, precluding the use of same-site controls (Rice et al., 1997). This differs from axonal release in striatum that exhibits stable release levels with repetitive stimulation (e.g., Chen and Rice, 2001), in part because of more efficient DA uptake in striatum than SNc, which facilitates reuptake and recycling of released DA (Cragg et al., 1997a). Here, as previously (Chen and Rice, 2001; Chen et al., 2006), we therefore evaluated regulation of somatodendritic DA release by comparing averaged pulse-train evoked $[DA]_o$ at two to four sites in the SNc on one side of a bisected midbrain slice with averaged paired recordings on the contralateral side in the presence of drug(s). The order of control and drug recordings was alternated between slice pairs. Data are expressed as a percentage of control responses, with the average maximum $[DA]_o$ evoked under control conditions taken as 100%.

Calcium imaging. Fluorescence imaging of $[Ca^{2+}]_i$ in single DAergic neurons was used to examine the time course of potentiation of $[Ca^{2+}]_i$ by caffeine Procedures for whole-cell recording (Avshalumov et al., 2005) and Ca^{2+} imaging with dye loading via pipettes used for whole-cell recording (Fedirko et al., 2007) were as described previously. Midbrain slices (300 μm thick) were allowed to recover for 30 min at 34°C in a solution containing (in mM): NaCl (125); KCl (2.5); $MgCl_2$ (1.0); $NaHCO_3$ (25); NaH_2PO_4 (1.25); glucose (25); ascorbate (1); pyruvate (3); $CaCl_2$ (2) at pH 7.3–7.4 and saturated with 95% O_2/5% CO_2. Slices were then cooled to room temperature and held for at least 30 min before experimentation. For recording, slices were transferred to a submersion chamber and maintained at 32°C while superfused with bicarbonate-buffered aCSF (as described in the previous section).

Current-clamp recordings from DAergic neurons in the SNc were obtained using an Axopatch 200B amplifier (Molecular Devices). These cells showed characteristic spontaneous pacemaker firing (1–5 Hz) and displayed a large inward rectification (i.e., a prominent sag) in response to hyperpolarizing steps (Yung et al., 1991; Wilson and Callaway, 2000; Avshalumov et al., 2005). The intracellular filling solution contained (in mM): K-gluconate (120); KCl (20); MgCl (2); Na-HEPES (10); EGTA (0.1); Na_2-ATP (2); GTP (0.2); pH adjusted to 7.2–7.3 with KOH, 280–290 mOsmol/L. The intracellular solution also contained Alexa Red 594 (0.1%), for cell visualization (Avshalumov et al., 2005) and Fluo-5F (300 μM), a medium-affinity (K_d of 1–2.3 μM) Ca^{2+} indicator for $[Ca^{2+}]_i$ imaging (Scott and Rusakov, 2006; Fedirko et al., 2007). The excitation wavelength for Fluo-5F was 475 nm with emission at 543 nm. Images were obtained using 2 × 2 binning with 500–700 ms exposure at 1 s intervals. A region of interest (ROI) was identified over the cell body. A background region adjacent to the recorded cell was also imaged; this background fluorescence was subtracted from the ROI for each frame in subsequent data analysis. The Fluo-5F baseline fluorescence (F_0) was defined as the average fluorescence obtained from 10 frames recorded immediately before drug application in each cell. Caffeine-induced changes in $[Ca^{2+}]_i$ are expressed as changes in Fluo-5F fluorescence over Fluo-5F baseline ($\Delta F/F_0 \times 100\%$). Paired statistical comparisons were made using the average fluorescence obtained from 10 frames recorded when the drug effect reached a maximum plateau (usually ~15 min).

Drugs and chemicals. All experimental solutions were prepared immediately before use. Components of the HEPES-buffer and bicarbonate-buffer solutions were obtained from Sigma-Aldrich Chemical Co., as were BAPTA-AM, DA, and caffeine. Cadmium (Cd^{2+}) chloride was from Fisher Scientific, 2-APB, CPCCOEt, cyclopiazonic acid (CPA), dantrolene and DHPG were from Tocris Bioscience, and Alexa Red and Fluo-5F were from Invitrogen.

Most drugs were water soluble and were prepared as aqueous stock solutions or dissolved directly in aCSF. However, stock solutions of 100 mM CPCCOEt, 2-APB and 50 mM BAPTA-AM, CPA were made in dimethyl sulfoxide (DMSO, Sigma-Aldrich). The final content of DMSO in aCSF was <0.1%; control data were obtained in the presence of the same concentration of DMSO and did not differ from control responses in aCSF alone. Most drugs were applied via the superfusing aCSF for ~40–50 min before recordings were made, except that caffeine and Cd^{2+} were applied for ~15 min and BAPTA-AM for ~30 min. In some experiments, pretreatment for the same duration at room temperature was used before exposure to a second agent in the recording chamber.

Statistical analysis. Data were analyzed using GraphPad Prism Software (GraphPad). Voltammetry and imaging data are expressed as means ± SEM; *n* is the number of slices for DA release data or number of cells for Ca^{2+} imaging with 2–3 slices or slice pairs per animal. Significance of differences presented was assessed using Student's *t* tests (paired or un-paired as appropriate) for comparison of the averaged peak response in drug versus control for both voltammetry and imaging data. For voltammetric data, similar results were also obtained when two-way ANOVA followed by Bonferroni's *post hoc* analysis was used to compare entire averaged $[DA]_o$ versus time profiles. The confidence level for significance was set at 95%.

Results

In the SN, DAergic somata and dendrites are readily identified by their immunoreactivity to antibodies against TH, the rate-limiting enzyme for DA synthesis (Rice et al., 1997). The SNc contains a dense intermingling of large TH immunoreactive (TH-ir) perikarya; each perikaryon gives rise to a few dendrites that extend laterally within the SNc, as well as ventrally into the SNr. In the SNr, TH immunostaining is restricted to long, ventrally extending dendrites. A useful feature of TH immunostaining is that it evenly labels all parts of the DAergic neuron, including its finest dendritic processes (Fig. 1*a*,*d*), which enabled us to examine TH-ir somata and dendrites for colocalization with proteins that regulate intracellular Ca^{2+} stores.

Proteins associated with intracellular Ca^{2+} regulation in SNc DAergic neurons

SERCA2 immunostaining

High levels of Ca^{2+} are maintained within intracellular ER stores by SERCA activity (Pozzan et al., 1994). There are three subtypes

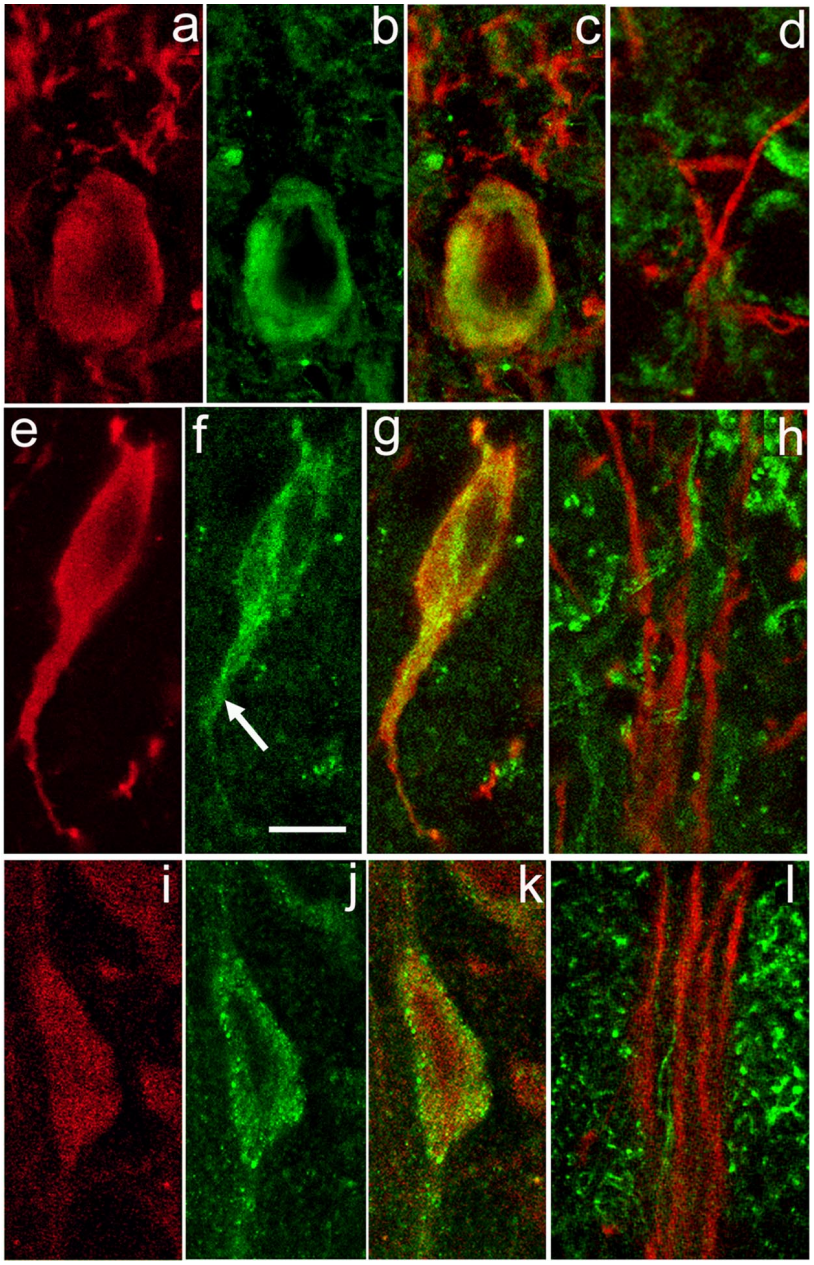

Figure 1. ER Ca^{2+} stores protein immunoreactivity in nigral DAergic neurons. ***a–c***, SERCA2 immunoreactivity in DAergic neurons in the SNc. Immunostaining for TH (red) (***a***) and SERCA2 (green) (***b***) with merged images for TH and SERCA (overlap appears yellow) (***c***). In the perikaryal cytoplasm, SERCA2 immunoreactivity is observed as a ring around the nucleus that extends almost to the perikaryal edge. Additional SERCA staining is seen within the most proximal portion of TH-ir dendrites (TH-ir profiles above perikaryon in ***c***). ***d***, However, SERCA staining is absent from DAergic dendrites within SNr. ***e–g***, Localization of IP_3Rs in DAergic neurons in the SNc. Immunostaining for TH (red) (***e***) and IP_3R (green) (***f***) with merged images for TH and IP_3R (***g***). Note that immunoreactivity to IP_3R and TH colocalizes in the perikaryon and extends down a proximal dendrite (***f***, arrow). ***h***, In SNr, however, IP_3R immunoreactivity (green) does not colocalize with that of TH (red), implying minimal IP_3R expression in distal DAergic dendrites. ***i–k***, Localization of RyRs in DAergic neurons in the SNc. Immunostaining for TH (red) (***i***) and RyR (green) (***j***) with merged images for TH and RyR (***k***). Note that RyR immunostaining includes a mixture of large puncta located at the edge of the perikaryon and smaller puncta located in the perikaryal cytoplasm. ***l***, RyR immunoreactivity (green) does not colocalize with that of TH within SNr, implying low levels in distal dendrites. Scale bar: (in ***f***) ***a–l***, 10 μm.

of SERCA of which SERCA2 is the predominant neuronal subtype (Baba-Aissa et al., 1996; Verkhratsky, 2005). To examine the presence of SERCA in DAergic neurons, we used a pan antibody that recognizes the two isoforms of SERCA2: SERCA2a and SERCA2b. The cellular distribution of this and other proteins presented in this report was assessed using *z*-axis scans. Illustrated images for each protein are from a single level of a representative *z*-stack. Immunostaining for SERCA2 in the SNc and SNr indicated abundant expression in DAergic neurons, as well as in non-DAergic cells known to be present in the SN (Nair-Roberts et al., 2008). Within the DAergic perikarya, prominent SERCA2 immunoreactivity was observed in a band of cytosol surrounding the cell nucleus and extending almost to the perikaryal periphery (Fig. 1*a–c*). This band was not uniform in staining intensity, but rather showed patches of higher and lower immunoreactivity (Fig. 1*b*). SERCA2 staining diminished rapidly in intensity within the proximal portions of DAergic dendrites (Fig. 1*c*), with a lack of detectable SERCA2 in distal dendrites (Fig. 1*d*).

IP_3R immunostaining

The IP_3R is activated through a metabotropic cascade and governs Ca^{2+} release from intracellular ER stores (Foskett et al., 2007). We found that IP_3R immunostaining was punctate, consisting of small grains of uniform size that had a relatively homogeneous distribution throughout the cytoplasm of DAergic perikarya and their proximal dendrites (Fig. 1*e–g*). For comparison of IP_3R immunostaining patterns in a distinct neuronal population, we tested the same IP_3R antibody in the cerebellum and found a similarly even distribution of IP_3R throughout the cytoplasm of Purkinje cell somata and apical dendrites, as described previously for a different IP_3R antibody used in rat Purkinje cells (Sharp et al., 1993). Like SERCA2, IP_3R staining was not visible in distal portions of DAergic dendrites within the SNr (Fig. 1*h*).

RyR immunostaining

The RyR is typically activated by a rise in $[Ca^{2+}]_i$ and gates Ca^{2+} release from ER stores (Verkhratsky and Shmigol, 1996; Fill and Copello, 2002). There are three isoforms of RyRs that are differentially distributed throughout the CNS. Using a pan RyR antibody that recognizes all three RyR isoforms, we found an unusual distribution of RyR immunostaining within TH-ir somata (Fig. 1*i–k*). In DAergic neurons, RyR staining was punctate, with the striking presence of large puncta, 0.4–0.8 μm in diameter, that were preferentially distributed at the margin of the cell body adjacent to the plasma membrane. We also observed smaller puncta, ~0.3 μm in diameter, that were distributed throughout the perikaryal cytoplasm. Immunoreactivity for RyR was also observed in proximal TH-ir dendrites, but was not visible in distal DAergic dendrites extending into SNr (Fig. 1*l*). To examine whether the localization of larger, membrane-associated RyR puncta was a common neuronal feature, we ex-

amined RyR immunostaining in guinea-pig cerebellar Purkinje cells. In contrast to DAergic neurons of the SNc, RyR immunoreactivity in Purkinje cells consisted exclusively of small puncta that were distributed homogeneously throughout the perikaryal cytoplasm (not illustrated), as reported previously for rat Purkinje cells (Sharp et al., 1993). This comparison not only verifies that the presence of larger RyR puncta is not an artifact of our protocol, but also suggests a specific functional role for RyRs adjacent to the membrane of DAergic somata in the SNc.

mGluR1α immunostaining

Nigral DAergic neurons receive glutamatergic input from the subthalamic nucleus (Chang et al., 1984; Kita and Kitai, 1987; Rinvik and Ottersen, 1993; Iribe et al., 1999) and pedunculopontine nucleus (Charara et al., 1996; Smith et al., 1996), that can activate both ionotropic and metabotropic glutamatergic receptors. Metabotropic mGluR1 activation may be particularly important because it couples to IP_3 production that can mobilize Ca^{2+} from IP_3R-gated ER stores (Pin and Duvoisin, 1995; Conn and Pin, 1997). There are multiple isoforms of mGluR1s, of which mGluR1α is among the most widely distributed in the brain. Previous studies suggest that mGluR1α is strongly expressed in SNc DAergic neurons in monkeys (Hubert et al., 2001; Kaneda et al., 2003) and mice (Nakamura et al., 2004), but is either weakly expressed or absent in DAergic neurons in rats (Kosinski et al., 1998; Testa et al., 1998; Hubert et al., 2001). Interestingly, we found that mGluR1α was present in DAergic neurons of the guinea-pig SNc. The staining pattern for mGluR1α immunoreactivity consisted of puncta that were particularly dense near the edge of DAergic perikaryon, as determined in *z*-axis scans (Fig. 2*a–c*), which showed abundant mGluR1α staining in DAergic somata, with moderate levels of mGluR1α puncta in DAergic dendrites within SNc (Fig. 2*a–c*) and those extending into the SNr (Fig. 2*d–f*).

Ca_v1.3 immunostaining

A trigger for RyR-dependent CICR is Ca^{2+} entry via VGCCs (Verkhratsky and Shmigol, 1996). Moreover, there is evidence for functional coupling between RyRs and L-type Ca^{2+} channels (Chavis et al., 1996; Mouton et al., 2001). These channels are also of particular importance for SNc DAergic neurons, because they carry the major Ca^{2+} current that drives

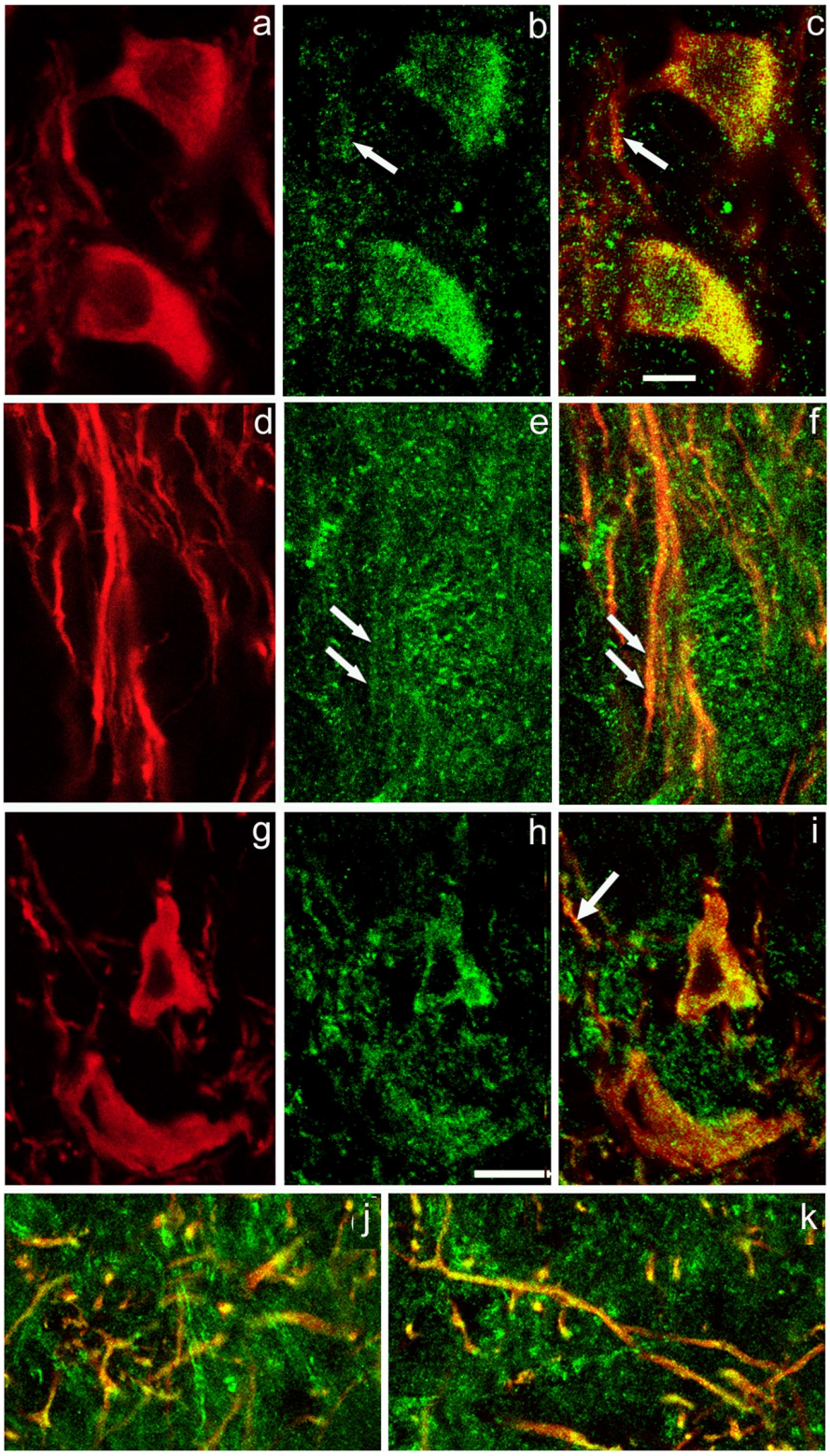

Figure 2. mGluR1α and Ca_v1.3 immunoreactivity in nigral DAergic neurons. ***a–c***, Immunostaining for TH (red) (***a***) and mGluR1α (green) (***b***) with merged images for TH and mGluR1α (overlap appears yellow) (***c***). The mGluR1α immunoreactivity appears as puncta that colocalize with TH in the perikarya and primary dendrites of DAergic neurons in SNc. Arrows in ***b*** and ***c*** indicate corresponding locations at which colocalization of mGluR1α immunoreactivity and TH immunoreactivity occurs in dendritic processes within SNc. ***d–f***, A moderate level of mGluR1α staining is seen within TH-ir dendrites in SNr. Paired arrows in ***e*** and ***f*** point to colocalization of mGluR1α and TH immunoreactivity in a dendritic profile. ***g–i***, Localization of Ca_v1.3, an L-type Ca^{2+} channel subunit, in DAergic neuronal perikarya in the SNc. Immunostaining for TH (red) (***g***) and Ca_v1.3 (green) (***h***) with merged images for TH and Ca_v1.3 (***i***). Ca_v1.3 immunoreactivity is punctate. ***j***, ***k***, Colocalization of immunoreactivity to TH and Ca_v1.3 in DAergic processes at the border of SNc/SNr (***j***) and deep within SNr (***k***). Scale bar: (in ***c***) ***a–f***, 10 μm; (in ***h***) ***g–k***, 20 μm.

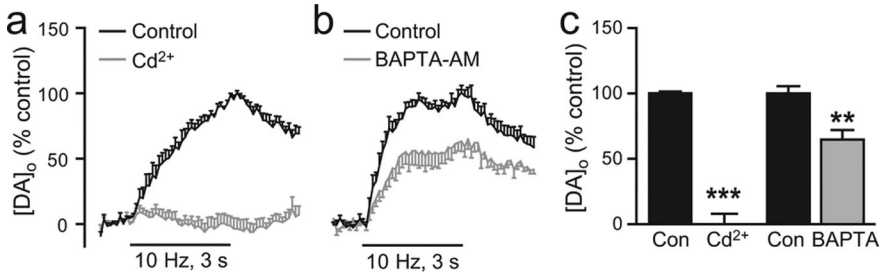

Figure 3. Ca^{2+} entry and intracellular Ca^{2+} facilitate somatodendritic DA release. ***a***, Average $[DA]_o$ versus time profiles evoked by local stimulation (30 pulses, 10 Hz) in the SNc in the absence and presence of a nonselective Ca^{2+} channel blocker, Cd^{2+} (100 μM, $n = 6$). ***b***, Average $[DA]_o$ versus time profiles in SNc in the absence and presence of a fast-acting Ca^{2+} chelator BAPTA-AM (BAPTA) (50 μM, $n = 6$). ***c***, Summary of the effect of Cd^{2+} and BAPTA on peak $[DA]_o$; evoked $[DA]_o$ was measured at the time point of control peak $[DA]_o$, which was taken as 100%. Blockade of stimulus-induced Ca^{2+} entry by Cd^{2+} abolished evoked $[DA]_o$ ($n = 6$, $^{***}p < 0.001$ vs control), confirming that Ca^{2+} entry is required to trigger evoked somatodendritic DA release. Buffering of stimulus-induced intracellular Ca^{2+} by BAPTA decreased evoked $[DA]_o$ ($n = 6$, $^{**}p < 0.01$ vs control), demonstrating the involvement of intracellular Ca^{2+} elevation in evoked somatodendritic DA release.

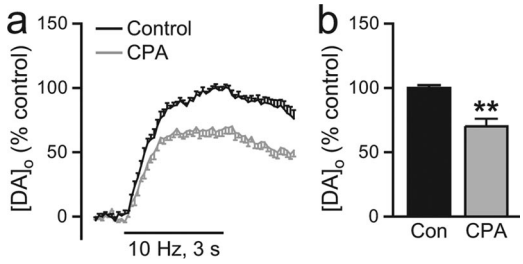

Figure 4. Effect of SERCA inhibition on somatodendritic DA release. ***a***, Average $[DA]_o$ versus time profiles in the SNc evoked by local stimulation (30 pulses, 10 Hz) in the absence and presence of a membrane-permeable SERCA inhibitor, CPA (30 μM, $n = 6$). ***b***, Summary of the effect of CPA on peak $[DA]_o$; control peak $[DA]_o$ was taken as 100%. Inhibition of SERCA by CPA decreased evoked $[DA]_o$ ($n = 6$, $^{**}p < 0.01$ vs control), demonstrating the involvement of ER Ca^{2+} stores in somatodendritic DA release.

the characteristic pacemaker activity of these cells (Wilson and Callaway, 2000; Choi et al., 2003; Durante et al., 2004; Puopolo et al., 2007; Surmeier, 2007). A previous study by Takada et al. (2001) showed that in rat SNc, an L-type VGCC, $Ca_v1.3$ (also called α1D), is abundantly expressed throughout DAergic neuronal somata and dendrites. We also found $Ca_v1.3$-ir puncta in TH-ir perikarya (Fig. 2*g–i*) confirming the presence of these channels in DAergic neurons of guinea-pig SNc. In addition, abundant $Ca_v1.3$-ir puncta were found in DAergic dendrites at the SNc/SNr border (Fig. 2*j*), as well as in dendrites located wholly within SNr (Fig. 2*k*). Additional $Ca_v1.3$-ir puncta, were noted in processes of other, non-DAergic neurons.

Dependence of somatodendritic DA release on Ca^{2+} entry and $[Ca^{2+}]_i$ elevation

To assess the functional roles of ER store proteins in somatodendritic DA release in the SNc, we used fast-scan cyclic voltammetry with carbon-fiber microelectrodes. Average $[DA]_o$ evoked by local pulse-train stimulation (30 pulses at 10 Hz) in the SNc in 2.4 mM $[Ca^{2+}]_o$ was 0.38 ± 0.02 μM ($n = 78$, pooled from all control recordings). Evoked $[DA]_o$ was detectable after the first few stimulus pulses and remained elevated throughout the stimulus. With this stimulation paradigm, evoked $[DA]_o$ in the SNc is TTX- and reserpine-sensitive, and persists in the presence of a DA uptake inhibitor, implying that evoked somatodendritic DA release is exocytotic and does not occur via reversal of the DA transporter (Cragg et al., 1997a; Rice et al., 1997; Chen and Rice, 2001). However, DA release in the SNc under these conditions is insensitive to inhibition by a mixture of VGCC blockers applied at concentrations sufficient to prevent axonal DA release in the striatum (Chen et al., 2006). The persistence of DA release in SNc under these conditions presumably reflects the incomplete blockade of VGCCs, coupled with the minimal Ca^{2+} entry required for initiation of somatodendritic DA release.

The question of which VGCCs are involved in somatodendritic DA release therefore remains unresolved. Indeed, Mendez et al. (2008) recently reported that N- and P/Q-type channels mediate basal DA release measured by radioimmunoassay in mesencephalic cultures, whereas Kim et al. (2008) found that blockade of L- and T-type channels, but not N- or P/Q-type channels decreases the frequency of K^+-induced exocytotic events detected by amperometry in dissociated DAergic cells. Given this ambiguity, here we simply sought to clarify the dependence of evoked somatodendritic DA release on Ca^{2+} entry using the nonselective Ca^{2+} channel blocker Cd^{2+} (100 μM). Evoked DA release in the SNc was abolished by Cd^{2+} ($p < 0.001$ vs control, $n = 6$) (Fig. 3*a*,*c*), demonstrating that somatodendritic DA release indeed requires Ca^{2+} entry.

To examine whether an increase in $[Ca^{2+}]_i$ also is involved in somatodendritic DA release, we used the fast acting intracellular Ca^{2+} chelator BAPTA-AM to buffer stimulus-evoked changes in $[Ca^{2+}]_i$. BAPTA-AM is inactive in the extracellular environment; however once this membrane-permeable chelator enters cells, the AM group is cleaved by intracellular esterases to form active BAPTA. A previous study showed that at 50 μM, BAPTA-AM caused a ~35% decrease in the frequency and amplitude of mEPSCs recorded from pyramidal cells in slices of rat barrel cortex, implying attenuation, but not elimination of $[Ca^{2+}]_i$ transients (Simkus and Stricker, 2002). We found that 50 μM BAPTA-AM also caused a similar decrease in evoked $[DA]_o$ ($p < 0.01$, $n = 6$) (Fig. 3*b*,*c*), implicating $[Ca^{2+}]_i$ elevation in the somatodendritic DA release process.

Intracellular Ca^{2+} stores and somatodendritic DA release regulation

SERCA

Our immunocytochemical studies showed abundant labeling of SERCA2 in SNc DAergic neurons (Fig. 1*a–c*). Therefore, to determine whether SERCA-sensitive Ca^{2+} stores are involved in somatodendritic DA release, we examined the effect of SERCA inhibition on evoked $[DA]_o$ in the SNc. We found that a membrane-permeable SERCA inhibitor, CPA (30 μM) (Seidler et al., 1989), decreased evoked $[DA]_o$ by ~40% ($p < 0.01$, $n = 6$) (Fig. 4*a*,*b*), demonstrating the involvement of intracellular ER Ca^{2+} stores in somatodendritic DA release.

IP_3R-gated stores

We also identified the presence of IP_3Rs throughout the cytoplasm of SNc DAergic somata (Fig. 1*e–g*). To assess the potential role of IP_3Rs in somatodendritic DA release, we first tested a membrane-permeable IP_3R antagonist, 2-APB (100 μM; Maruyama et al., 1997). Consistent with a role for Ca^{2+} release from IP_3R-sensitive stores in DAergic neurons, we found that 2-APB

caused a ~60% decrease ($p < 0.001$, $n = 8$) in evoked $[DA]_o$ (Fig. 5*a*,*b*). Having thus established involvement of IP_3Rs in somatodendritic DA release, we next examined a potential source of IP_3 generation: activation of mGluR1s. These metabotropic glutamate receptors are present on both the somata and dendrites of SNc DAergic neurons (Fig. 2*a–f*). Moreover, previous studies have shown that activation of mGluR1s regulates membrane excitability via mobilization of Ca^{2+} from IP_3R-dependent stores in SNc DAergic neurons (Fiorillo and Williams, 1998; Morikawa et al., 2003). We therefore tested the hypothesis that mGluR1 activation also modulates evoked DA release. Indeed, we found that a low concentration of an mGluR1 agonist, DHPG (1 μM), caused a ~25% increase in evoked $[DA]_o$ ($p < 0.05$, $n = 8$) (Fig. 5*c*,*d*). In contrast, when a much higher concentration of DHPG (200 μM) was used, this enhancement was lost (100 ± 2% for control responses vs 103 ± 12% for DHPG, $p > 0.05$, $n = 6$) (not illustrated).

We then examined whether mGluR1s are activated by endogenously released glutamate during local stimulation, using a selective noncompetitive mGluR1 antagonist, CPCCOEt (100 μM) (Hermans et al., 1998). Blockade of mGluR1s with CPCCOEt decreased evoked $[DA]_o$ by ~45% ($p < 0.001$, vs paired control, $n = 9$) (Fig. 5*c*,*d*), suggesting that endogenous glutamate enhances somatodendritic DA release by mGluR1 activation.

Confirming the involvement of IP_3R-gated stores in the activation of mGluR1s by endogenous glutamate, we found that suppression of evoked DA release by CPCCOEt was prevented by pretreatment with the IP_3R antagonist, 2-APB (100 μM) ($p > 0.05$ CPCCOEt + 2-APB vs 2-APB alone, $n = 6$) (Fig. 5*e*,*f*) or the SERCA inhibitor CPA (30 μM) ($p > 0.05$ CPCCOEt + CPA vs CPA alone, $n = 6$) (Fig. 5*e*,*f*). Thus regulation of somatodendritic DA release by endogenous glutamate acting at mGluR1s involves mobilization of Ca^{2+} from IP_3R-gated stores.

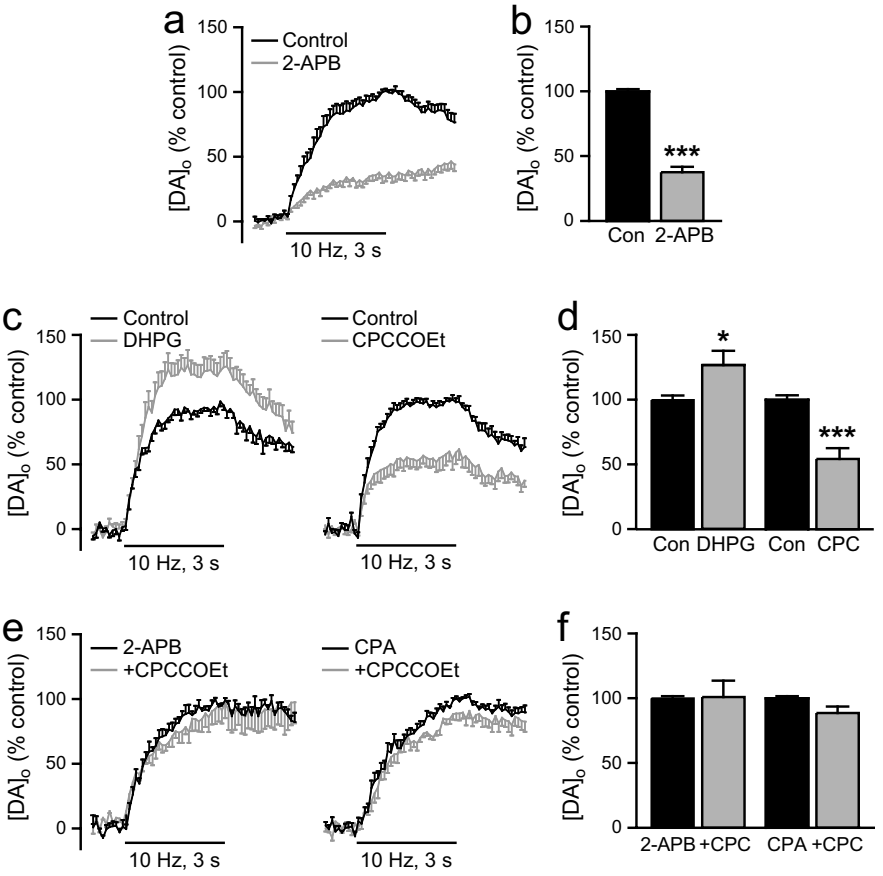

Figure 5. Regulation of somatodendritic DA release by mGluR1 activation of IP_3R-gated intracellular Ca^{2+} stores. ***a***, Average $[DA]_o$ versus time profiles in SNc evoked by local stimulation (30 pulses, 10 Hz) in the absence and presence of a membrane-permeable IP_3R inhibitor, 2-APB (left) (100 μM, $n = 8$). ***b***, Summary of the effect of 2-APB on peak $[DA]_o$; control peak $[DA]_o$ (Con) was taken as 100%. Inhibition of IP_3Rs by 2-APB decreased evoked $[DA]_o$ ($n = 8$, $^{***}p < 0.001$ vs control), indicating involvement of Ca^{2+} mobilization from IP_3R-gated stores in somatodendritic DA release. ***c***, Average $[DA]_o$ versus time profiles in SNc in the absence and presence of an mGluR1 agonist DHPG (left) (1 μM, $n = 8$) or the mGluR1 antagonist CPCCOEt (right) (100 μM, $n = 9$). ***d***, Summary of the effect of DHPG and CPCCOEt (CPC) on peak $[DA]_o$; control peak $[DA]_o$ was taken as 100%. Activation of the IP_3R-dependent mGluR1 pathway by DHPG significantly increased evoked $[DA]_o$ ($n = 8$, $^{*}p < 0.05$ vs control), implicating a role for mGluR1-gated Ca^{2+} stores in somatodendritic DA release. Blockade of mGluR1s with CPCCOEt decreased evoked $[DA]_o$ ($n = 9$, $^{***}p < 0.001$), indicating that endogenously released glutamate normally facilitates somatodendritic DA release via activation of mGluR1s. ***e***, Average $[DA]_o$ versus time profiles in SNc with CPCCOEt (100 μM) after pretreatment with the IP_3R antagonist 2-APB (left) (100 μM, $n = 6$) or the SERCA inhibitor CPA (right) (30 μM, $n = 6$). ***f***, Summary of the effect of CPCCOEt in 2-APB or CPA on peak $[DA]_o$; control peak $[DA]_o$ in either 2-APB or CPA alone was taken as 100%. Suppression of evoked $[DA]_o$ by CPCCOEt was prevented by pretreatment with 2-APB ($n = 6$, $p > 0.05$, CPC + 2-APB vs 2-APB alone) or CPA ($n = 6$, $p > 0.05$, CPC + CPA vs CPA alone), demonstrating that activation of mGluR1s by endogenously released glutamate involves mobilization of Ca^{2+} from IP_3R-gated ER stores.

Ryanodine receptor-gated Ca^{2+} stores

Our immunostaining revealed the presence of RyRs at the plasma membrane of SNc DAergic somata (Fig. 1*i–k*). This specialized distribution suggests that RyRs are well positioned for activation by minimal Ca^{2+} entry. To examine the possible functional role of RyRs in somatodendritic DA release, we first used caffeine to activate RyR-sensitive Ca^{2+} stores (Rousseau and Meissner, 1989; Sitsapesan and Williams, 1990; Avidor et al., 1994; Verkhratsky, 2005). For these studies we used 5 mM caffeine, which exceeds the K_D of ~1.5 mM for caffeine-induced Ca^{2+} release from ER stores (Hoesch et al., 2001). We monitored changes in $[Ca^{2+}]_i$ using the fluorescent indicator Fluo-5F in electrophysiologically identified SNc DAergic neurons to confirm the efficacy of 5 mM caffeine and to establish its time course of action. Because DAergic neurons are spontaneously active *in vitro*, these experiments were conducted in the presence of TTX (1 μM) to prevent depolarization-induced increases in $[Ca^{2+}]_i$, and in nominally zero $[Ca^{2+}]_o$ to abolish spontaneous Ca^{2+} oscillations, either of which might mask changes induced by caffeine. In addition, the use of TTX and zero $[Ca^{2+}]_o$ ensured that any changes in $[Ca^{2+}]_i$ were the result of mobilization of Ca^{2+} from stores within DAergic neurons and not a consequence of indirect changes via altered synaptic input. Under these conditions we found that caffeine increased $[Ca^{2+}]_i$ within a few minutes of application and reached a maximum effect of 143 ± 2% ($p < 0.01$ vs baseline, $n = 3$) within 15 min (Fig. 6*a*).

This Ca^{2+}-mobilizing concentration of caffeine (5 mM for ≥15 min) also caused a ~60% increase in evoked $[DA]_o$ ($p <$

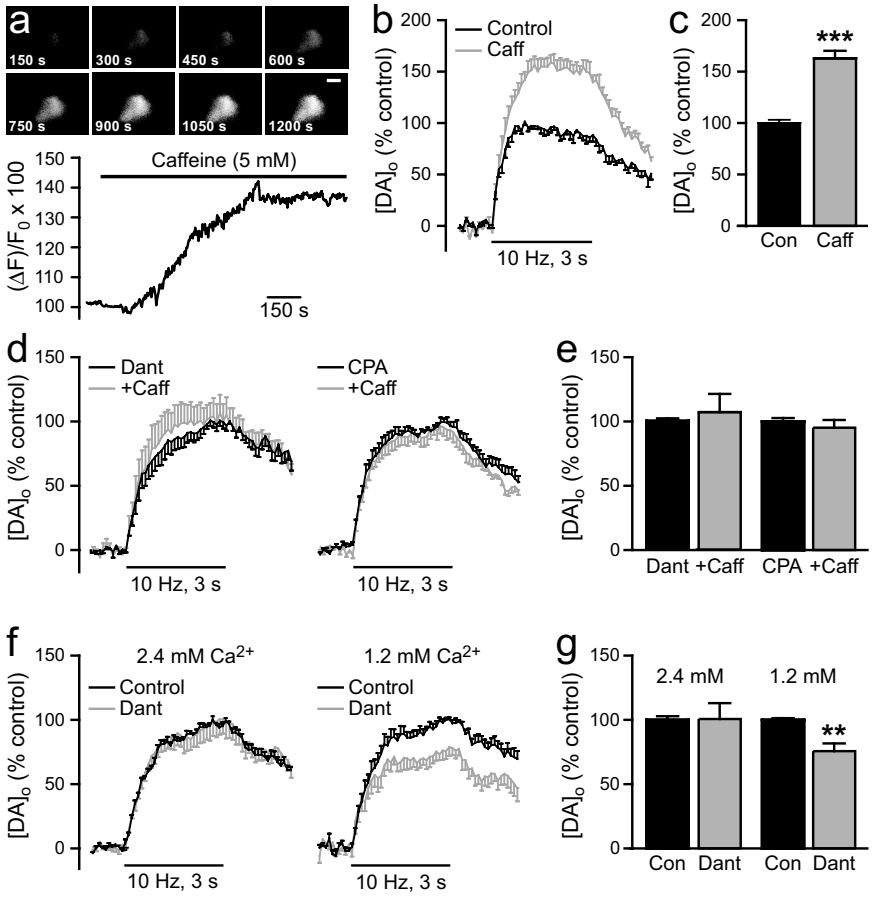

Figure 6. Regulation of somatodendritic DA release by RyR-gated intracellular Ca^{2+} stores. ***a***, Representative record of Fluo-5F fluorescence during RyR-activation by caffeine (5 mM), showing the time course of the resultant increase in $[Ca^{2+}]_i$ in an SNc DAergic neuron. Recordings were made in nominally zero $[Ca^{2+}]_o$ and in the presence of TTX (1 μM). ***b***, Average $[DA]_o$ versus time profiles in the SNc evoked by local stimulation (30 pulses, 10 Hz) in the absence and presence of caffeine (Caff) (5 mM, $n = 6$). ***c***, Summary of the effect of caffeine on peak $[DA]_o$; control peak $[DA]_o$ (Con) was taken as 100%. Activation of RyRs by caffeine increased evoked $[DA]_o$ ($n = 6$, ***$p < 0.001$ vs control), implicating RyR-gated Ca^{2+} stores in somatodendritic DA release. ***d***, Average $[DA]_o$ versus time profiles in SNc with caffeine (5 mM) after pretreatment with dantrolene (Dant) (10 μM), a RyR blocker (left, $n = 8$) or CPA (30 μM), a SERCA inhibitor (right, $n = 6$). ***e***, Summary of the effect of caffeine in dantrolene or CPA on peak $[DA]_o$; control peak $[DA]_o$ in either dantrolene or CPA alone was taken as 100%. Enhancement of evoked $[DA]_o$ by caffeine is prevented by pretreatment with dantrolene ($n = 8$, $p > 0.05$, Caff + Dant vs Dant alone) or CPA ($n = 6$, $p > 0.05$, Caff + CPA vs CPA alone), confirming the involvement of release of Ca^{2+} from RyR-gated stores in caffeine-mediated somatodendritic DA release. ***f***, Average $[DA]_o$ versus time profiles in SNc in the absence and presence of dantrolene (10 μM) in 2.4 mM $[Ca^{2+}]_o$ (left, $n = 8$) and 1.2 mM $[Ca^{2+}]_o$ (right, $n = 8$). ***g***, Summary of the effect of dantrolene on peak $[DA]_o$; control peak $[DA]_o$ was taken as 100%. Although dantrolene had little effect on evoked $[DA]_o$ in 2.4 mM $[Ca^{2+}]_o$ ($n = 8$, $p > 0.05$ vs control), a significant decrease in evoked $[DA]_o$ was revealed when dantrolene was applied in 1.2 mM $[Ca^{2+}]_o$ ($n = 8$, **$p < 0.01$ vs control), implicating RyR activation in somatodendritic DA release.

0.001, $n = 6$) (Fig. 6*b*,*c*), whereas a lower concentration of caffeine (250 μM) was without effect (100 ± 4% for control responses vs 110 ± 16% for caffeine; $p > 0.05$, $n = 7$) (not illustrated). The lack of effect of 250 μM provided an important control, because this concentration can have other effects including inhibition of cyclic nucleotide phosphodiesterase (Beavo and Reifsnyder, 1990) and blockade of adenosine receptors (Fisone et al., 2004; Cauli and Morelli, 2005). The increase in evoked $[DA]_o$ induced by 5 mM caffeine was prevented by an RyR blocker, dantrolene (10 μM) (Zhao et al., 2001) ($p > 0.05$, $n = 8$) (Fig. 6*d*,*e*), or by pretreatment with the SERCA inhibitor CPA (30 μM; $p > 0.05$, $n = 6$) (Fig. 6*d*,*e*), confirming the involvement of ER Ca^{2+} stores via activation of RyRs by caffeine.

Surprisingly, we found that application of dantrolene alone did not significantly alter evoked $[DA]_o$ in the presence of 2.4 mM $[Ca^{2+}]_o$ ($p > 0.05$, $n = 8$) (Fig. 6*f*,*g*), implying a lack of RyR involvement under these conditions. We hypothesized that this might reflect either sufficient Ca^{2+} entry to initiate DA release without RyR amplification of $[Ca^{2+}]_i$ or the dominance of IP_3R activation in the competition between RyRs and IP_3Rs for mobilization of a common Ca^{2+} store (Petersen et al., 2001). To assess these possible mechanisms, we first halved $[Ca^{2+}]_o$ to 1.2 mM, which would both decrease Ca^{2+} entry and suppress glutamate release and might thereby reveal a role for RyR-gated stores. Indeed, in 1.2 mM $[Ca^{2+}]_o$, dantrolene caused an ~25% suppression of evoked $[DA]_o$ ($p < 0.01$ vs paired control, $n = 8$) (Fig. 6*f*,*g*). To determine whether this was caused by masking of RyR involvement by glutamate-dependent activation of mGluR1-IP_3R-gated stores in higher $[Ca^{2+}]_o$, we returned to 2.4 mM $[Ca^{2+}]_o$ to examine the effect of dantrolene when mGluR1s were blocked by CPCCOEt. Again, however, dantrolene failed to suppress evoked DA release in 2.4 mM $[Ca^{2+}]_o$ even when mGluR1s were blocked ($p > 0.05$, $n = 9$), suggesting that under those conditions Ca^{2+} entry alone was sufficient to trigger DA release. Together these data indicate that endogenous activation and mobilization of Ca^{2+} from RyR-gated stores play important roles in amplifying somatodendritic DA release under conditions of minimal Ca^{2+} entry, but that sufficient Ca^{2+} entry obviates the need for RyR-dependent amplification of $[Ca^{2+}]_i$ to support optimal release.

Discussion

Somatodendritic DA release in the SN is essential for basal ganglia-mediated movement (Robertson and Robertson 1989; Timmerman and Abercrombie 1996; Crocker 1997; Bergquist et al., 2003). Most obviously, somatodendritic DA acting at D2 autoreceptors can inhibit DAergic neuron activity (Lacey et al., 1987; Pucak and Grace, 1994; Falkenburger et al., 2001; Beckstead et al., 2004), with consequent inhibition of both somatodendritic and axonal DA release (Santiago and Westerink 1991a,b). Somatodendritic DA also acts at postsynaptic DA receptors on GABAergic neurons in the SNr (Waszczak, 1990), as well as presynaptic DA receptors to regulate local release of GABA and glutamate (Waszczak and Walters, 1986; Miyazaki and Lacey 1998; Radnikow and Misgeld 1998; Hatzipetros and Yamamoto, 2006). However, factors that regulate somatodendritic DA release remain poorly understood.

The present study provides the first evidence for the involvement of IP_3R- and RyR-sensitive ER Ca^{2+} stores in the regulation of somatodendritic DA release. Immunocytochemical analysis revealed the presence of key proteins involved in Ca^{2+}-store regulation, including SERCA, IP_3Rs, and RyRs in guinea-pig SNc

DAergic neurons. Voltammetric experiments demonstrated the functionality of these proteins, including enhancement of somatodendritic DA release by endogenous glutamate acting at IP_3R-coupled mGluR1s and suppression of DA release by RyR blockade.

Ca^{2+} entry, ER Ca^{2+} stores, and transmitter release

Classical exocytosis requires a local increase in $[Ca^{2+}]_i$ from a basal level of ~100 nM to >100 μM (Llinás et al., 1992), which is typically achieved in presynaptic terminals by Ca^{2+} entry. Here we confirm that Ca^{2+} entry and $[Ca^{2+}]_i$ elevation are also required to initiate somatodendritic DA release, with abolition of release by Cd^{2+} and suppression by BAPTA-AM. However, the persistence of somatodendritic (DA) release under conditions of low $[Ca^{2+}]_o$ or partial VGCC blockade sufficient to abolish axonal release in striatum (Chen and Rice, 2001; Chen et al., 2006) suggests that amplification of $[Ca^{2+}]_i$ by Ca^{2+} mobilization from intracellular stores is also involved. Previous studies of Ca^{2+} stores in DA release regulation focused exclusively on axon terminals, however, and data from those studies are conflicting (Oyamada et al., 1998; Zhang and Sulzer, 2003; Fernandes et al., 2004; Zhu et al., 2004).

Our first evidence for Ca^{2+}-store involvement in somatodendritic DA release was that SERCA inhibition by CPA decreased evoked $[DA]_o$ (Fig. 4). Release of ER Ca^{2+} is proportional to the amount of Ca^{2+} stored (Petersen et al., 2001; Pozzan et al., 1994), which is maintained by SERCA; inhibition of SERCA results in store depletion. The inhibitory effect of CPA on evoked $[DA]_o$, therefore, indicates that Ca^{2+} release from ER stores normally amplifies DA release. These results complement data showing that ER Ca^{2+} stores can contribute to axonal, somatic, and dendritic release of other transmitters (Krizaj et al., 1999, Emptage et al., 2001; Bardo et al., 2002; Ludwig et al., 2002; Simkus and Stricker, 2002; Galante and Marty, 2003; Trueta et al., 2004). Intriguingly, anatomical studies have shown that neuronal ER forms a continuous system extending from soma to axons and presynaptic terminals, as well as to dendrites and dendritic spines (Solovyova and Verkhratsky, 2003; Bouchard et al., 2003; Verkhratsky, 2005). In SNc DAergic neurons, Ca^{2+} from somatic ER stores is propagated through this network to dendrites (Choi et al., 2006). This may obviate the need for an additional mechanism to maintain Ca^{2+} stores in dendrites, consistent with the diminishing presence of SERCA2 from somata to distal dendrites of DAergic neurons (Fig. 1*a–d*).

mGluR1 activation facilitates somatodendritic DA release via IP_3Rs

In contrast to differential SERCA distribution between somata and dendrites, mGluR1α is abundantly expressed in both compartments of TH-ir neurons in guinea-pig SNc, as also seen in other species (Hubert et al., 2001; Kaneda et al., 2003; Nakamura et al., 2004). Previous physiological studies in DAergic neurons indicate that mGluR1 activation by agonist application or transient synaptic glutamate release initiates IP_3R-mediated Ca^{2+} release from ER stores (Fiorillo and Williams, 1998; Morikawa et al., 2003). We show here that a key consequence of mGluR1 activation can be to facilitate somatodendritic DA release.

Previous studies have shown that mGluR1 activation can have biphasic effects depending on agonist concentration or stimulus intensity. For example, activation of mGluR1s by 1 μM DHPG in SNc DAergic neurons amplifies action potential-dependent increases in $[Ca^{2+}]_i$ via ER Ca^{2+} stores, whereas 30 μM DHPG depletes Ca^{2+} stores and suppresses subsequent Ca^{2+} mobilization (Cui et al., 2007). In striatum, strong activation of mGluR1s by either 200 μM DHPG or glutamate spillover during high-frequency stimulation inhibits axonal DA release (Zhang and Sulzer, 2003). Consistent with these effects, we found that activation of mGluR1s with 1 μM DHPG enhanced pulse-train evoked DA release in SNc, whereas this enhancing effect was lost with stronger activation by 200 μM DHPG.

More importantly, we show that mGluR1 activation by endogenous glutamate enhances somatodendritic DA release, indicated by suppression of evoked $[DA]_o$ by the mGluR1 antagonist CPCCOEt (Fig. 5). This was prevented by the IP_3R antagonist 2-APB and by the SERCA inhibitor CPA, implicating IP_3R-sensitive ER stores, with a caveat that 2-APB, like other available IP_3R inhibitors, can have additional actions, including SERCA inhibition (Missiaen et al., 2001; Peppiatt et al., 2003). Given robust evidence for mGluR1 coupling to IP_3 production (Pin and Duvoisin, 1995; Conn and Pin, 1997) and IP_3-dependent mobilization of ER Ca^{2+} in DAergic neurons (Morikawa et al., 2000; 2003), our data suggest that endogenous glutamate release facilitates somatodendritic DA release via mGluR1s coupled to Ca^{2+} release from IP_3R-sensitive stores. Interestingly, locally released glutamate acting via ionotropic NMDA and AMPA receptors in the SNc suppresses somatodendritic DA release by enhancing GABAergic input to DAergic neurons (Chen and Rice, 2002). As the net consequence of stimulation of glutamatergic input to the SN from the subthalamic nucleus *in vivo* is to enhance nigral $[DA]_o$ (Mintz et al., 1986), direct mGluR1-dependent facilitation of somatodendritic DA release may dominate over indirect inhibition via NMDA and AMPA receptors.

RyRs facilitate somatodendritic DA release

Immunocytochemical examination of RyRs in SNc DAergic neurons revealed larger RyR puncta near the surface of the cell than elsewhere in the cytoplasm (Fig. 1). The simplest explanation for these larger puncta at the plasma membrane is RyR clustering, which has been shown to be critical for the generation of Ca^{2+}'sparks' (Groff and Smith, 2008). Implicating a functional role for RyR-sensitive Ca^{2+} stores in the excitability of SNc DAergic neurons, blockade of RyRs by dantrolene decreases basal $[Ca^{2+}]_i$ and nearly abolishes spontaneous Ca^{2+} spike activity (Tsuneki et al., 2000). These observations are complemented by our findings that activation of RyRs by caffeine not only increased $[Ca^{2+}]_i$ in DAergic neurons, but also enhanced evoked $[DA]_o$ in a SERCA- and RyR-dependent manner (Fig. 6).

Endogenous activation of RyRs after Ca^{2+} entry also facilitates somatodendritic DA release, indicated by the suppression of evoked $[DA]_o$ by dantrolene in 1.2 mM $[Ca^{2+}]_o$, albeit not in 2.4 mM $[Ca^{2+}]_o$. In contrast to IP_3R-gated stores that require activation of G-protein-coupled receptors and IP_3 production, RyR-mediated CICR occurs rapidly with activation-time constants of <1 ms (Fill and Copello, 2002; Verkhratsky, 2005). The location of RyRs at the plasma membrane of DAergic neurons further suggests that RyRs are poised for rapid activation by minimal Ca^{2+} entry, resulting in CICR. This amplification mechanism could underlie the persistence of somatodendritic DA release in low $[Ca^{2+}]_o$ (Hoffman and Gerhardt, 1999; Chen and Rice, 2001; Fortin et al., 2006). Consistent with this notion, the distribution of $Ca_v1.3$ in DAergic somata parallels that of surface RyRs (Figs. 1*j,k*, 2*h,i*). Moreover, L-type Ca^{2+} channels may couple functionally to neuronal RyRs (Chavis et al., 1996; Mouton et al., 2001). This raises the possibility of depolarization-induced Ca^{2+} release via RyRs, even in the absence of Ca^{2+} entry, although prevention of DA release by Cd^{2+} argues against such direct

activation in our studies. However, the inability of dantrolene to suppress DA release in 2.4 mM $[Ca^{2+}]_o$ suggests that RyR amplification is unnecessary when sufficient transmembrane Ca^{2+} flux for DA release is available.

Conclusion and implications

We show here that glutamatergic input to SNc DAergic neurons can facilitate somatodendritic DA release through activation of mGluR1s and IP_3Rs and that DA release can also be amplified via RyR activation. Interestingly, our immunocytochemical data suggest that involvement of intracellular Ca^{2+} stores in DA release regulation may differ between somata and proximal dendrites in SNc and distal dendrites in SNr. The apparently even distribution of $Ca_v1.3$, for example, throughout DAergic somata and dendrites, coupled with low levels of SERCA, IP_3Rs, and RyRs in distal DAergic dendrites in SNr, suggest that Ca^{2+} entry via VGCCs into the compact dendritic compartment may be sufficient to promote DA release without the need for $[Ca^{2+}]_i$ amplification.

Overall, these data provide a new understanding of somatodendritic DA release by illuminating factors that underlie normal release regulation. The findings also have implications for pathological conditions. For example, in Parkinson disease, glutamatergic output neurons of the subthalamic nucleus are hyperactive (Lozano et al., 1998). Among other consequences of excessive glutamatergic input to SNc, persistent mGluR1 activation could deplete ER Ca^{2+} stores and suppress somatodendritic DA release, thereby exacerbating consequences of progressive DAergic neuron loss.

References

Avidor T, Clementi E, Schwartz L, Atlas D (1994) Caffeine-induced transmitter release is mediated via ryanodine-sensitive channel. Neurosci Lett 165:133–136.

Avshalumov MV, Chen BT, Koós T, Tepper JM, Rice ME (2005) Endogenous hydrogen peroxide regulates the excitability of midbrain dopamine neurons via ATP-sensitive potassium channels. J Neurosci 25:4222–4231.

Baba-Aissa F, Raeymaekers L, Wuytack F, De Greef C, Missiaen L, Casteels R (1996) Distribution of the organellar Ca^{2+} transport ATPase SERCA2 isoforms in the cat brain. Brain Res 743:141–153.

Bardo S, Robertson B, Stephens GJ (2002) Presynaptic internal Ca^{2+} stores contribute to inhibitory transmitter release onto mouse cerebellar Purkinje cells. Br J Pharmacol 137:529–537.

Beavo JA, Reifsnyder DH (1990) Primary sequence of cyclic nucleotide phosphodiesterase isoenzymes and the design of selective inhibitors. Trends Pharmacol Sci 11:150–155.

Beckstead MJ, Grandy DK, Wickman K, Williams JT (2004) Vesicular dopamine release elicits an inhibitory postsynaptic current in midbrain dopamine neurons. Neuron 42:939–946.

Beltramino CA, Forbes MS, Swanson DJ, Alheid GF, Heimer L (1996) Amygdaloid input to transiently tyrosine hydroxylase immunoreactive neurons in the bed nucleus of the stria terminalis of the rat. Brain Res 706:37–46.

Bergquist F, Ludwig M (2008) Dendritic transmitter release: a comparison of two model systems. J Neuroendocrinol 20:677–686.

Bergquist F, Niazi HS, Nissbrandt H (2002) Evidence for different exocytosis pathways in dendritic and terminal dopamine release in vivo. Brain Res 950:245–253.

Bergquist F, Shahabi HN, Nissbrandt H (2003) Somatodendritic dopamine release in rat substantia nigra influences motor performance on the accelerating rod. Brain Res 973:81–91.

Björklund O, Lindvall O (1975) Dopamine in dendrites of substantia nigra neurons: suggestions for a role in dendritic terminals. Brain Res 83:531–537.

Bouchard R, Pattarini R, Geiger JD (2003) Presence and functional significance of presynaptic ryanodine receptors. Prog Neurobiol 69:391–418.

Bourguignon LY, Jin H, Iida N, Brandt NR, Zhang SH (1993) The involvement of ankyrin in the regulation of inositol 1,4,5-trisphosphate receptor-mediated internal Ca^{2+} release from Ca^{2+} storage vesicles in mouse T-lymphoma cells. J Biol Chem 268:7290–7297.

Cauli O, Morelli M (2005) Caffeine and the dopaminergic system. Behav Pharmacol 16:63–77.

Chang HT, Kita H, Kitai ST (1984) The ultrastructural morphology of the subthalamic-nigral axon terminals intracellularly labeled with horseradish peroxidase. Brain Res 299:182–185.

Charara A, Smith Y, Parent A (1996) Glutamatergic inputs from the pedunculopontine nucleus to midbrain dopaminergic neurons in primates: phaseolus vulgaris-leucoagglutinin anterograde labeling combined with postembedding glutamate and GABA immunohistochemistry. J Comp Neurol 364:254–266.

Chavis P, Fagni L, Lansman JB, Bockaert J (1996) Functional coupling between ryanodine receptors and L-type calcium channel in neurons. Nature 382:719–722.

Chen BT, Rice ME (2001) Novel Ca^{2+} dependence and time course of somatodendritic dopamine release: substantia nigra versus striatum. J Neurosci 21:7841–7847.

Chen BT, Rice ME (2002) Synaptic regulation of somatodendritic dopamine release by glutamate and GABA differs between substantia nigra and ventral tegmental area. J Neurochem 81:158–169.

Chen BT, Moran KA, Avshalumov MV, Rice ME (2006) Limited regulation of somatodendritic dopamine release by voltage-sensitive Ca^{2+} channels contrasted with strong regulation of axonal dopamine release. J Neurochem 96:645–655.

Cheramy A, Leviel V, Glowinski J (1981) Dendritic release of dopamine in the substantia nigra. Nature 289:537–542.

Choi YM, Kim SH, Uhm DY, Park MK (2003) Glutamate-mediated $[Ca^{2+}]_c$ dynamics in spontaneously firing dopamine neurons of the rat substantia nigra pars compacta. J Cell Science 116:2665–2675.

Choi YM, Kim SH, Chung S, Uhm DY, Park MK (2006) Regional interaction of endoplasmic reticulum Ca^{2+} signals between soma and dendrites through rapid luminal Ca^{2+} diffusion. J Neurosci 26:12127–12136.

Conn PJ, Pin JP (1997) Pharmacology and functions of metabotropic glutamate receptors. Annu Rev Pharmacol Toxicol 37:205–237.

Cragg SJ, Rice ME, Greenfield SA (1997a) Heterogeneity of electrically evoked dopamine release and reuptake in substantia nigra, ventral tegmental area and striatum. J Neurophysiol 77:863–873.

Cragg SJ, Hawkey CR, Greenfield SA (1997b) Comparison of serotonin and dopamine release in substantia nigra and ventral tegmental area: region and species differences. J Neurochem 69:2378–2386.

Crocker AD (1997) The regulation of motor control: an evaluation of the role of dopamine receptors in the substantia nigra. Rev Neurosci 8:55–76.

Cui G, Bernier BE, Harnett MT, Morikawa H (2007) Differential regulation of action potential- and metabotropic glutamate receptor-induced Ca^{2+} signals by inositol 1,4,5-triphosphate in dopamine neurons. J Neurosci 27:4776–4785.

Durante P, Cardenas CG, Whittaker JA, Kitai ST, Scroggs RS (2004) Low-threshold L-type calcium channels in rat dopamine neurons. J Neurophysiol 91:1450–1454.

Elverfors A, Jonason J, Jonason G, Nissbrandt H (1997) Effects of drugs interfering with sodium channels and calcium channels on the release of endogenous dopamine from superfused substantia nigra slices. Synapse 26:359–369.

Emptage NJ, Reid CA, Fine A (2001) Calcium stores in hippocampal synaptic boutons mediate short-term plasticity, store-operated Ca^{2+} entry, and spontaneous transmitter release. Neuron 29:197–208.

Falkenburger BH, Barstow KL, Mintz IM (2001) Dendrodendritic inhibition through reversal of dopamine transport. Science 293:2465–2470.

Fedirko N, Avshalumov M, Rice ME, Chesler M (2007) Regulation of postsynaptic Ca^{2+} influx in hippocampal CA1 pyramidal neurons via extracellular carbonic anhydrase. J Neurosci 27:1167–1175.

Fernandes VM, Romano-Silva MA, Gomes DA, Prado MA, Santos TM, Gomez MV (2004) Dopamine release evoked by beta scorpion toxin, tityus gamma, in prefrontal cortical slices is mediated by intracellular calcium stores. Cell Mol Neurobiol 24:757–767.

Fill M, Copello JA (2002) Ryanodine receptor calcium release channels. Physiol Rev 82:893–922.

Fiorillo CD, Williams JT (1998) Glutamate mediates an inhibitory postsynaptic potential in dopamine neurons. Nature 394:78–82.

Fisone G, Borgkvist A, Usiello A (2004) Caffeine as a psychomotor stimulant: mechanism of action. Cell Mol Life Sci 61:857–872.

Fortin GD, Desrosiers CC, Yamaguchi N, Trudeau LE (2006) Basal somatodendritic dopamine release requires snare proteins. J Neurochem 96:1740–1749.

Foskett JK, White C, Cheung KH, Mak DO (2007) Inositol trisphosphate receptor Ca^{2+} release channels. Physiol Rev 87:593–658.

Galante M, Marty A (2003) Presynaptic ryanodine-sensitive calcium stores contribute to evoked neurotransmitter release at the basket cell-Purkinje cell synapse. J Neurosci 23:11229–11234.

Geffen LB, Jessell TM, Cuello AC, Iversen LL (1976) Release of dopamine from dendrites in rat substantia nigra. Nature 260:258–260.

Groff JR, Smith GD (2008) Ryanodine receptor allosteric coupling and the dynamics of calcium sparks. Biophys J 95:135–154.

Hatzipetros T, Yamamoto BK (2006) Dopaminergic and GABAergic modulation of glutamate release from rat subthalamic nucleus afferents to the substantia nigra. Brain Res 1076:60–67.

Heeringa MJ, Abercrombie ED (1995) Biochemistry of somatodendritic dopamine release in substantia nigra: an in vivo comparison with striatal dopamine release. J Neurochem 65:192–200.

Hell JW, Westenbroek RE, Warner C, Ahlijanian MK, Prystay W, Gilbert MM, Snutch TP, Catterall WA (1993) Identification and differential subcellular localization of the neuronal class C and class D L-type calcium channel alpha 1 subunits. J Cell Biol 123:949–962.

Hermans E, Nahorski SR, Challiss RA (1998) Reversible and non-competitive antagonist profile of CPCCOEt at the human type 1α metabotropic glutamate receptor. Neuropharmacology 37:1645–1647.

Hoesch RE, Weinreich D, Kao JP (2001) A novel Ca^{2+} influx pathway in mammalian primary sensory neurons is activated by caffeine. J Neurophysiol 86:190–196.

Hoffman AF, Gerhardt GA (1999) Differences in pharmacological properties of dopamine release between the substantia nigra and striatum: an in vivo electrochemical study. J Pharmacol Exp Ther 289:455–463.

Hubert GW, Paquet M, Smith Y (2001) Differential subcellular localization of mGluR1a and mGluR5 in the rat and monkey substantia nigra. J Neurosci 21:1838–1847.

Iravani MM, Kruk ZL (1997) Real-time measurement of stimulated 5-hydroxytryptamine release in rat substantia nigra pars reticulata brain slices. Synapse 25:93–102.

Iribe Y, Moore K, Pang KC, Tepper JM (1999) Subthalamic stimulation-induced synaptic responses in substantia nigra pars compacta dopaminergic neurons in vitro. J Neurophysiol 82:925–933.

Jaffe EH, Marty A, Schulte A, Chow RH (1998) Extrasynaptic vesicular transmitter release from the somata of substantia nigra neurons in rat midbrain slices. J Neurosci 18:3548–3553.

John CE, Budygin EA, Mateo Y, Jones SR (2006) Neurochemical characterization of the release and uptake of dopamine in ventral tegmental area and serotonin in substantia nigra of the mouse. J Neurochem 96:267–282.

Kaneda K, Imanishi M, Nambu A, Shigemoto R, Takada M (2003) Differential expression patterns of mGluR1 alpha in monkey nigral dopamine neurons. Neuroreport 14:947–950.

Kim Y, Park MK, Chung S (2008) Voltage-operated Ca^{2+} channels regulate dopamine release from somata of dopamine neurons in the substantia nigra pars compacta. Biochem Biophys Res Commun 373:665–669.

Kita H, Kitai ST (1987) Efferent projections of the subthalamic nucleus in the rat: light and electron microscopic analysis with the PHA-L method. J Comp Neurol 260:435–452.

Kosinski CM, Standaert DG, Testa CM, Penny JB Jr, Young AB (1998) Expression of metabotropic glutamate receptor isoforms in the substantia nigra pars compacta of the rat. Neuroscience 86:783–798.

Koulen P, Kuhn R, Wässle H, Brandstätter JH (1997) Group I metabotropic glutamate receptors mGluR1alpha and mGluR5a: localization in both synaptic layers of the rat retina. J Neurosci 17:2200–2211.

Kriegsfeld LJ, Mei DF, Yan L, Witkovsky P, Lesauter J, Hamada T, Silver R (2008) Targeted mutation of the calbindin D28K gene disrupts circadian rhythmicity and entrainment. Eur J Neurosci 27:2907–2921.

Krizaj D, Bao JX, Schmitz Y, Witkovsky P, Copenhagen DR (1999) Caffeine-sensitive calcium stores regulate synaptic transmission from retinal rod photoreceptors. J Neurosci 19:7249–7261.

Lacey MG, Mercuri NB, North RA (1987) Dopamine acts on D2 receptors to increase potassium conductance in neurones of the rat substantia nigra zona compacta. J Physiol 392:397–416.

Llinás R, Sugimori M, Silver RB (1992) Microdomains of high calcium concentration in a presynaptic terminal. Science 256:677–679.

Lozano AM, Lang AE, Hutchison WD, Dostrovsky JO (1998) New developments in understanding the etiology of Parkinson's disease and in its treatment. Curr Opin Neurobiol 8:783–790.

Ludwig M, Sabatier N, Bull PM, Landgraf R, Dayanithi G, Leng G (2002) Intracellular calcium stores regulate activity-dependent neuropeptide release from dendrites. Nature 418:85–89.

Maruyama T, Kanaji T, Nakade S, Kanno T, Mikoshiba K (1997) 2APB, 2-Aminoethixydiphenyl borate, a membrane-penetrable modulator of Ins(1,4,5)P_3-induced Ca^{2+} release. J Biochem 122:498–505.

Mendez J, Bourque MJ, Trudeau LE (2008) Somatodendritic dopamine release requires synaptotagmin 4 and 7 and the participation of voltage-gated calcium channels. Soc Neurosci Abstr 34:34.11.

Millar J, Pelling CW (2001) Improved methods for construction of carbon fibre electrodes for extracellular spike recording. J Neurosci Methods 110:1–8.

Mintz I, Hammond C, Guibert B, Leviel V (1986) Stimulation of the subthalamic nucleus enhances the release of dopamine in the rat substantia nigra. Brain Res 25:406–408.

Missiaen L, Callewaert G, De Smedt H, Parys JB (2001) 2-Aminoethoxydiphenyl borate affects the inositol 1,4,5-trisphosphate receptor, the intracellular Ca^{2+} pump and the non-specific Ca^{2+} leak from the non-mitochondrial Ca^{2+} stores in permeabilized A7r5 cells. Cell Calcium 29:111–116.

Miyazaki T, Lacey MG (1998) Presynaptic inhibition by dopamine of a discrete component of GABA release in rat substantia nigra pars reticulata. J Physiol 513:805–817.

Morikawa H, Imani F, Khodakhah K, Williams JT (2000) Inositol 1,4,5-triphosphate-evoked responses in midbrain dopamine neurons. J Neurosci 20:RC103(1–5).

Morikawa H, Khodakhah K, Williams JT (2003) Two intracellular pathways mediate metabotropic glutamate receptor-induced Ca^{2+} mobilization in dopamine neurons. J Neurosci 23:149–157.

Mouton J, Marty I, Villaz M, Feltz A, Maulet Y (2001) Molecular interaction of dihydropyridine receptors with type-1 ryanodine receptors in rat brain. Biochem J 354:597–603.

Nair-Roberts RG, Chatelain-Badie SD, Benson E, White-Cooper H, Bolam JP, Ungless MA (2008) Stereological estimates of dopaminergic, GABAergic and glutamatergic neurons in the ventral tegmental area, substantia nigra and retrorubral field in the rat. Neuroscience 152:1024–1031.

Nakamura M, Sato K, Fukaya M, Araishi K, Aiba A, Kano M, Watanabe M (2004) Signaling complez formation of phospholipase Cβ4 with metabotropic glutamate receptor type 1α and 1,4,5-trisphosphate receptor at the perisynapse and the endoplasmic reticulum in the mouse brain. Eur J Neurosci 20:2929–2944.

Nieoullon A, Cheramy A, Glowinski J (1977) Release of DA *in vivo* from cat SN. Nature 266:375–377.

Oyamada T, Hayashi T, Kagaya A, Yokota N, Yamawaki S (1998) Effect of dantrolene on K^+- and caffeine-induced dopamine release in rat striatum assessed by microdialysis. Neurochem Int 32:171–176.

Patel J, Rice ME (2006) Dopamine release in brain slices. In: Encyclopedia of sensors, Vol 6 (Grimes CA, Dickey EC, Pishko MV, eds), pp 313–334. Stevenson Ranch, CA: American Scientific.

Peppiatt CM, Collins TJ, Mackenzie L, Conway SJ, Holmes AB, Bootman MD, Berridge MJ, Seo JT, Roderick HL (2003) 2-Aminoethoxydiphenyl borate (2-APB) antagonizes inositol 1,4,5-trisphosphate-induced calcium release, inhibits calcium pumps and has use-dependent and slowly reversible action on store-operated calcium entry channels. Cell Calcium 34:97–108.

Petersen OH, Tepikin A, Park MK (2001) The endoplasmic reticulum: one continuous or several separate Ca^{2+} stores? Trends Neurosci 24:271–276.

Pin JP, Duvoisin R (1995) The metabotropic glutamate receptors: structure and functions. Neuropharmacology 34:1–26.

Pozzan T, Rizzuto R, Volpe P, Meldolesi J (1994) Molecular and cellular physiology of intracellular calcium stores. Physiol Rev 74:595–636.

Pucak ML, Grace AA (1994) Evidence that systemically administered dopamine antagonists activate dopamine neuron firing primarily by blockade of somatodendritic autoreceptors. J Pharmacol Exp Ther 271:1181–1192.

Puopolo M, Raviola E, Bean BP (2007) Roles of subthreshold calcium current and sodium current in spontaneous firing of mouse midbrain dopamine neurons. J Neurosci 27:645–656.

Radnikow G, Misgeld U (1998) Dopamine D_1 receptors facilitate $GABA_A$ synaptic currents in the rat substantia nigra pars reticulata. J Neurosci 18:2009–2016.

Rice ME, Richards CD, Nedergaard S, Hounsgaard J, Nicholson C, Greenfield SA (1994) Direct monitoring of dopamine and 5-HT release in substantia nigra and ventral tegmental area *in vitro*. Exp Brain Res 100:395–406.

Rice ME, Cragg SJ, Greenfield SA (1997) Characteristics of electrically evoked somatodendritic dopamine release in substantia nigra and ventral tegmental area *in vitro*. J Neurophysiol 77:853–862.

Rinvik E, Ottersen OP (1993) Terminals of the subthalamonigral fibres are enriched with glutamate-like immunoreactivity: an electron microscopic, immunogold analysis in the cat. J Chem Neuroanat 6:19–30.

Robertson GS, Robertson HA (1989) Evidence that l-Dopa-induced rotational behavior is dependent on both striatal and nigral mechanisms. J Neurosci 9:3326–3331.

Robertson GS, Damsma G, Fibiger HC (1991) Characterization of dopamine release in the substantia nigra by *in vivo* microdialysis in freely moving rats. J Neurosci 11:2209–2216.

Rousseau E, Meissner G (1989) Single cardiac sarcoplasmic reticulum Ca^{2+} release channel: activation by caffeine. Am J Physiol 256:H328–H333.

Santiago M, Westerink BH (1991a) Characterization and pharmacological responsiveness of dopamine release recorded by microdialysis in the substantia nigra of conscious rats. J Neurochem 57:738–747.

Santiago M, Westerink BH (1991b) The regulation of dopamine release from nigrostriatal neurons in conscious rats: the role of somatodendritic autoreceptors. Eur J Pharmacol 204:79–85.

Santiago M, Machado A, Cano J (1992) Fast sodium channel dependency of the somatodendritic release of dopamine in the rat's brain. Neurosci Lett 148:145–147.

Scott R, Rusakov DA (2006) Main determinants of presynaptic Ca^{2+} dynamics at individual mossy fiber CA3 pyramidal cell synapses. J Neurosci 26:7071–7081.

Seidler NW, Jona I, Vegh M, Martonosi A (1989) Cyclopiazonic acid is a specific inhibitor of the Ca^{2+}-ATPase of sarcoplasmic reticulum. J Biol Chem 264:17816–17823.

Sharp AH, McPherson PS, Dawson TM, Aoki C, Campbell KP, Snyder SH (1993) Differential immunohistochemical localization of inositol 1,4,5-triphosphate- and ryanodine-sensitive Ca^{2+} release channels in rat brain. Neuroscience 13:3051–3063.

Simkus CR, Stricker C (2002) The contribution of intracellular calcium stores to mEPSCs recorded in layer II neurons of the rat barrel cortex. J Physiol 545:521–535.

Sitsapesan R, Williams AJ (1990) Mechanisms of caffeine activation of single calcium-release channels of sheep cardiac sarcoplasmic reticulum. J Physiol 423:425–439.

Smith Y, Charara A, Parent A (1996) Synaptic innervation of midbrain dopaminergic neurons by glutamate-enriched terminals in the squirrel monkey. J Comp Neurol 364:231–253.

Solovyova N, Verkhratsky A (2003) Neuronal endoplasmic reticulum acts as a single functional Ca^{2+} store shared by ryanodine and inositol-1,4,5-triphosphate receptors as revealed by intra-ER $[Ca^{2+}]$ recordings in single rat sensory neurons. Pflugers Arch 446:447–454.

Stutzmann GE, Smith I, Caccamo A, Oddo S, Laferla FM, Parker I (2006) Enhanced ryanodine receptor recruitment contributes to Ca^{2+} disruptions in young, adult, and aged Alzheimer's disease mice. J Neurosci 26:5180–5189.

Surmeier DJ (2007) Calcium, ageing, and neuronal vulnerability in Parkinson's disease. Lancet Neurol 6:933–938.

Takada M, Kang Y, Imanishi M (2001) Immunohistochemical localization of voltage-gated calcium channels in substantia nigra dopamine neurons. Eur J Neurosci 13:757–762.

Testa CM, Friberg IK, Weiss SW, Standaert DG (1998) Immunohistochemical localization of metabotropic glutamate receptors mGluR1a and mGluR2/3 in the rat basal ganglia. J Comp Neurol 390:5–19.

Timmerman W, Abercrombie ED (1996) Amphetamine-induced release of dendritic dopamine in substantia nigra pars reticulata: D1-mediated behavioral and electrophysiological effects. Synapse 23:280–291.

Trueta C, Sánchez-Armass S, Morales MA, De-Miguel FF (2004) Calcium-induced calcium release contributes to somatic secretion of serotonin in leech Retzius neurons. J Neurobiol 61:309–316.

Tsuneki H, Klink R, Léna C, Korn H, Changeux JP (2000) Calcium mobilization elicited by two types of nicotinic acetylcholine receptors in mouse substantia nigra pars compacta. Eur J Neurosci 12:2475–2485.

Verkhratsky A (2005) Physiology and pathophysiology of the calcium store in the endoplasmic reticulum of neurons. Physiol Rev 85:201–279.

Verkhratsky A, Shmigol A (1996) Calcium-induced calcium release in neurons. Cell Calcium 19:1–14.

Waszczak BL (1990) Differential effects of D1 and D2 dopamine receptor agonists on substantia nigra pars reticulata neurons. Brain Res 513:125–135.

Waszczak BL, Walters JR (1986) Endogenous dopamine can modulate inhibition of substantia nigra pars reticulata neurons elicited by GABA iontophoresis or striatal stimulation. J Neurosci 6:120–126.

Wilson CJ, Callaway JC (2000) Coupled oscillator model of the dopamine neuron of the substantia nigra. J Neurophysiol 83:3084–3100.

Witkovsky P, Arango-Gonzalez B, Haycock JW, Kohler K (2005) Rat retinal dopaminergic neurons: differential maturation of somatodendritic and axonal compartments. J Comp Neurol 481:352–362.

Yung WH, Häusser MA, Jack JJ (1991) Electrophysiology of dopaminergic and non-dopaminergic neurons of the guinea-pig substantia nigra pars compacta in vitro. J Physiol 436:643–667.

Zhang H, Sulzer D (2003) Glutamate spillover in the striatum depresses dopaminergic transmission by activating group I metabotropic glutamate receptors. J Neurosci 23:10585–10592.

Zhao F, Li P, Chen SR, Louis CF, Fruen BR (2001) Dantrolene inhibition of ryanodine receptor Ca^{2+} release channels. Molecular mechanisms and isoform selectivity. J Biol Chem 276:13810–13816.

Zhu G, Okada M, Yoshida S, Hirose S, Kaneko S (2004) Both 3,4-dihydrophenylalanine and dopamine releases are regulated by Ca^{2+}-induced Ca^{2+} releasing system in rat striatum. Neurosci Lett 362:244–248.